f = approximate solution for indicated function, based on Eq. 1
$\langle\ \rangle$ = average over flow cross-section
$\binom{t}{r}$ = binomial coefficient

LITERATURE CITED

Abramowitz, M., and I. A. Stegun, eds., *Handbook of Mathematical Functions*, Dover (1972).

Aris, R., "On the Dispersion of a Solute in a Fluid Flowing Through a Tube," *Proc. Roy. Soc.* A, **235**, 67 (1956).

Campbell, G. A., and R. M. Foster, "Fourier Integrals for Practical Applications," D. Van Nostrand, Princeton, NJ (1967).

Chatwin, P. C. "The Approach to Normality of the Concentration Distribution of a Solute in a Solvent Flowing in a Straight Pipe," *J. Fluid Mech.*, **43**, 321 (1970).

Chatwin, P. C., "The Initial Development of Longitudinal Dispersion in Straight Tubes," *J. Fluid Mech.*, **80**, 33 (1977).

Damköhler, G., "Einflüsse der Strömung, Diffusion und Wärmeüberganges auf die Leistung von Reacktionsöfen. I. Allgemeine Gesichtspunkte für die Übertragung eines chemischen Prozesses aus dem Kleinen ins Grosse," *Z. Electrochem.*, **42**, 846 (1936).

De Gance, A. E., and L. E. Johns, "The Theory of Dispersion of Chemically Active Solutes in a Rectilinear Flow Field," *Appl. Sci. Res.*, **34**, 189 (1978a).

De Gance, A. E., and L. E. Johns, "On the Dispersion Coefficients for Poiseuille Flow in a Circular Cylinder," *Appl. Sci. Res.*, **34**, 227 (1978b).

Finlayson, B. A., *The Method of Weighted Residuals and Variational Principles*, Academic Press, New York (1972).

Gill, W. N., and R. Sankarasubramanian, "Exact Analysis of Unsteady Convective Diffusion," *Proc. Roy. Soc.* A, **316**, 341 (1970).

Gill, W. N., and R. Sankarasubramanian, "Dispersion of a Non-Uniform Slug in Time-Dependent Flow," *Proc. Roy. Soc.* A, **322**, 101 (1971).

Lighthill, J. M., "Initial Development of Diffusion in Poiseuille Flow," *J. Inst. Math. Applics.*, **2**, 97 (1966).

Sankarasubramanian, R., and W. N. Gill, "Unsteady Convective Diffusion with Interphase Mass Transfer," *Proc. Roy. Soc.* A, **333**, 115 (1973); **341**, 407 (1974).

Taylor, G., "Dispersion of Soluble Matter in Solvent Flowing Slowly Through a Tube," *Proc. Roy. Soc.* A, **219**, 186 (1953).

Villadsen, J. V., and M. L. Michelsen, *Solutions of Differential Equation Models by Polynomial Approximation*, Prentice-Hall, Englewood Cliffs, NJ (1978).

Villadsen, J. V., and W. E. Stewart, "Solution of Boundary-Value Problems by Orthogonal Collocation," *Chem. Eng. Sci.*, **22**, 1483 (1967); **23**, 1515 (1968).

Manuscript received October 6, 1981; revision received and accepted September 15, 1982.

Particulate Deposition from Turbulent Parallel Streams

KWAN H. IM and PAUL M. CHUNG

Argonne National Laboratory
Argonne, IL 60439

A theory is developed for the rate of particulate deposition from turbulent gas streams onto surfaces. Three characteristic times—the particle relaxation time, the turbulent fluctuation time, and the particle residence time—control the deposition mode. Two phenomena are primarily responsible for transport of the particles across the laminar sublayer and deposition: 1) the momentum imparted to the particle by the fluid turbulence; and 2) the thermospheresis caused by the temperature gradient near the wall. Interaction of the three characteristic times with these two phenomena is analyzed, and the particle deposition rate in turbulent pipe flow is computed. The findings are found to be in close agreement with available experimental data.

SCOPE

Successful design of much industrial equipment such as certain heat exchanger surfaces requires understanding the mechanisms of mass transfer from the particle- or droplet-laden gas streams to solid surfaces. Particulate (or droplet) deposition on surfaces is caused by three different mechanisms, depending largely on the particle relaxation time and the turbulent fluctuation time. The particle relaxation time is proportional to the square of the particle diameter and to the material density of the particle, and is inversely proportional to the fluid viscosity. The very large particles, for which the relaxation time is much longer than the turbulent fluctuation time, impinge on surfaces that cross their mean trajectories. Therefore, in a parallel flow, capture of these particles is rare.

Smaller particles, for which the relaxation time is of the order of or smaller than the turbulent fluctuation time, diffuse across the mean streamlines toward the wall because of the fluid turbulence. The larger particles among these, for which the relaxation time is of the order of the turbulent fluctuation time, gain sufficient turbulence momentum to carry them across the laminar sublayer and result in wall deposition. For the particle material densities of the order of 2,000 kg/m^3, these particles are approximately 1 to 10 μm in radius when the air is used as a carrier gas.

The momentum of the smaller particles, with relaxation time much smaller than the fluctuation time, dissipates in the sublayer; it is not sufficient to result in their capture on the wall. There are two phenomena that could extend the particulate migration to the wall; the Brownian motion and thermophoresis. The Brownian motion is inefficient; its contribution to the deposition can be neglected for all practical purposes (Fuchs, 1964). On the other hand, thermophoresis is an effective mechanism that causes diffusion of the submicron particles toward the colder surface when a temperature gradient is imposed across the laminar sublayer.

In the following, a theoretical model is constructed that describes the transport of particles from turbulent streams to

P. M. Chung is also at the University of Illinois in Chicago.

surfaces in parallel flows in general, and in pipe flows in particular. Turbulent transport to the vicinity of the laminar sublayer is first analyzed. Then, migration of the particles across the sublayer and to the surface by the turbulence-imparted momentum and thermophoresis is described. Finally, an expression for particulate deposition is constructed by combining the analyses of the turbulent diffusion and the two near-surface migration phenomena. Discussion of typical numerical results and comparison with available experimental data are then given.

CONCLUSION AND SIGNIFICANCE

Particulate deposition from turbulent streams onto solid surfaces is analyzed for parallel flows. The fluid turbulence causes particles to diffuse to the vicinity of the laminar sublayer. The effective diffusion velocity, Eq. 31, monotonically decreases as the particle size is increased. Therefore, the deposition rate approaches zero as the particle size increases according to the present theory.

Near the laminar sublayer, a portion of the fluid turbulence momentum is imparted to the particles. This momentum is sufficient for the larger particles to overcome dissipation through the laminar sublayer and reach the wall. For the smaller particles, on the other hand, the momentum is dissipated quickly, and the thermophoresis actuated by a temperature difference is needed to complete the journey. Both near-wall processes were analyzed and were combined with the turbulent diffusion analysis mentioned in the preceeding paragraph to construct a self-contained expression for the surface deposition rate. This expression shows that the deposition rate initially increases with particle size, but reaches a maximum. The rate then decreases toward zero as the particle size is continuously increased.

The particulate collection rate is rather strongly governed by the fluid turbulence. Therefore, it is sensitive to the Reynolds number and surface roughness that affect the turbulence. The capture rate of the smaller particles that need to be aided by thermophoresis can be substantially enhanced by increasing the temperature difference between the fluid and the wall.

Results of the present theory were found to compare satisfactorily in magnitude and trend with respect to the particle size, Reynolds number, and temperature difference with various experimental data for pipe flow.

TURBULENT TRANSPORT

The flow field in the pipe is divided into the three regions of fully-turbulent layer, buffer layer, and laminar sublayer for convenience, Figure 1. For the larger particles, the momentum imparted to them at distance S is sufficient to carry them to the surface. For the smaller particles, on the other hand, the thermophoretic force is needed for the completion of passage through the laminar sublayer.

A turbulent transport equation will be analyzed in this section, between $y = R$ and S, where $S \geq l$, with the particulate conditions at S undetermined. Behavior of the particles near the wall, $0 \leq y \leq S$, will be analyzed in the next section. A complete solution will then be constructed and the deposition rate will be determined by matching the analyses of the two regions at S in the subsequent sections.

The starting point of the analysis is the conservation equation of the particles,

$$u\frac{\partial c}{\partial x} - \frac{1}{(R-y)}\frac{\partial}{\partial y}\left[(R-y)\,D\frac{\partial c}{\partial y}\right] = 0, \tag{1}$$

where uniform size and properties are assumed for the particles. Boundary conditions for highly turbulent flow are specified as follows.

At $x = 0$,

$$c(0,y) = c_o = \text{constant} \tag{2}$$

At $y = S$,

$$D\frac{\partial c}{\partial y} = Vc = J \tag{3}$$

For $y \geq b$,

$$c = c_a \text{ and } u = u_a. \tag{4}$$

In Eq. 3, J is the particle flux toward the surface at S, which is not known *a priori*; in fact, J is the deposition rate being sought from the analysis. It will be determined by suitably matching the solution of Eq. 1 to the analysis of the particle behavior in $0 \leq y \leq S$. The stopping distance, S, is also an unknown and is related to the particle relaxation time and the fluid velocity fluctuations. It will be discussed in a subsequent section.

For convenience, solutions of Eq. 1 will be obtained in two segments: one for the fully turbulent region; the other for the buffer layer. For the fully turbulent region, Eq. 1 is put into the integral form

$$\frac{d}{dx}\int_b^R (R-y)ucdy + (R-b)D\left(\frac{\partial c}{\partial y}\right)_b = 0, \tag{5}$$

where the condition of Eq. 4 has been applied. In this region, u is nearly constant, and c is approximately uniform with respect to y. Equation 5, therefore, reduces to

$$u_a\frac{dc_a}{dx} = -\frac{2}{(R-b)}\left(D\frac{\partial c}{\partial y}\right)_b. \tag{6}$$

Integration with respect to y of Eq. 1 for the buffer layer results in

$$\frac{1}{2}(R-b)^2u_a\frac{dc_a}{dx} + \frac{d}{dx}\int_S^b uc(R-y)dy = -(R-S)\left(D\frac{\partial c}{\partial y}\right)_S, \tag{7}$$

where Eq. 6 has been used for $(D\partial c/\partial y)_b$. After Pohlhausen (see Schlichting), a suitable form for c-profile must be assumed to effect integration of Eq. 7.

For simplicity, we may assume the profile,

$$c(x,y) = A_1(x) + A_2(x)y. \tag{8}$$

where A_1 and A_2 are arbitrary functions to be determined in terms of the boundary conditions of Eqs. 3 and 4. However, this will result in a solution of Eq. 7 that will contain the diffusivity at $y = S$ only.

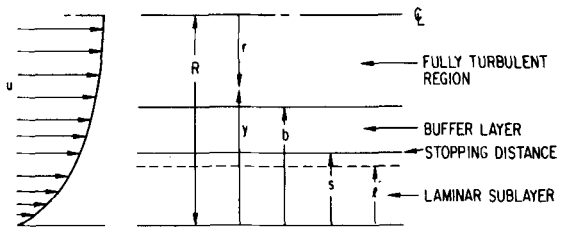

Figure 1. Sketch of flow regions.

Such overemphasis of the property values at a boundary is inherent in the Pohlhausen integral method.

This difficulty is circumvented and the variation of diffusivity across the buffer layer conveniently incorporated into the integral scheme by defining a modified ordinate as (Chung, 1966).

$$\eta = \int_S^y \frac{dy'}{D(y')}. \tag{9}$$

Then, we assume the profile as

$$c(x,y) = A_3(x) + A_4(x)\eta \tag{10}$$

instead of Eq. 8. Upon application of the boundary condition (Eq. 3), and the condition of $c(x,b) = c_a(x)$ at $y = b$, Eq. 10 becomes

$$c(x,y) = \left[\frac{1 + V/\hat{D}(y)}{1 + V/\hat{D}(b)}\right] c_a(x), \tag{11}$$

where the effective turbulent diffusion velocity, $\hat{D}(y)$, is defined as

$$\hat{D}(y) = 1/\eta = \left[\int_S^y \frac{dy'}{D(y')}\right]^{-1}. \tag{12}$$

V is the particle approach velocity toward the surface on which particles deposit. S is yet to be determined.

A substitution of the profile, Eq. 11, and the diffusion mass flux at $y = S$, Eq. 3, into Eq. 7 results in the equation,

$$\frac{d}{dx}(c_a F) + \frac{c_a V(R - S)}{1 + V/\hat{D}(b)} = 0, \tag{13}$$

where

$$F = \frac{1}{2}(R - b)^2 u_a + \int_S^b u(R - y)\left[\frac{1 + V/\hat{D}(y)}{1 + V/\hat{D}(b)}\right] dy. \tag{14}$$

The velocity u in the buffer layer is given by the usual logarithmic profile (Schlichting, 1968).

Equation 13 is formally integrated to give

$$c_a = c_o\left(\frac{F_o}{F}\right)\exp\left[-\int_0^x \frac{(R - S)V}{[1 + V/\hat{D}(b)]F}\, dx\right]. \tag{15}$$

Equation 11, with c_a given by Eq. 15, is the solution of Eq. 1 constructed up to one undetermined parameter, V. This parameter will be determined from the analysis of the $y \leqslant S$ region to be carried out subsequently.

It may be useful to discuss a physical aspect of the analysis carried out. Using Eqs. 11 and 12, Eq. 3 gives

$$\frac{J}{c_a} = \frac{1}{1/\hat{D}(b) + 1/V}. \tag{16}$$

J/c_a is the effective deposition velocity of the particles originating in the fully turbulent region with the mass concentration c_a. It is governed by both the turbulent transport and the particle behavior adjacent to the wall. On the righthand side of Eq. 16, $\hat{D}(b)$ as defined by Eq. 12 is the effective diffusion velocity of the particles across the buffer layer, and V is related to their migration velocity through the sublayer adjacent to the wall. In this sublayer, V is controlled by either the turbulence-imparted momentum or the action of thermophoresis. Equation 16 shows that, when there is much difference in the efficiencies of the two transport mechanisms (through the buffer layer, through the sublayer), the less efficient one becomes the controlling mechanism.

Note that the present concept of two mechanisms, one governing the fully turbulent region and the other governing the layer adjacent to the wall where the turbulence is not dominant, is analogous to that employed in the analysis of continuum plasma in Chung et al. (1975). The continuum plasma was considered to consist of the ambipolar region, where the molecular or turbulent transport was dominant, and the sheath adjacent to the wall, where the electric properties governed the electron and ion migration. There, also, a result basically similar to Eq. 16 was obtained.

Equations 11 and 15 show that expressions for $\hat{D}(y)$ and S, as well as V, are needed to complete the solution for the surface deposition. These will be discussed in the following sections.

PARTICLE DIFFUSION

An expression for the effective particulate diffusion velocity, $\hat{D}(b)$, is sought. The fluid eddy viscosities, ϵ, for the pipe flow and other parallel flows are rather well known (for instance, Cebeci and Smith, 1974; Ahluwalia and Doss, 1980). Therefore, it is only necessary to establish the relationship between the particulate eddy diffusivity, D, and the fluid eddy viscosity, ϵ. Specifically, the particulate Schmidt number, $Sc(\equiv \epsilon/D)$, is sought. The effective diffusion velocity, $\hat{D}(y)$, can then be constructed from Eq. 12 in terms of ϵ.

Assume, first, the standard fluid turbulent Schmidt number, $Sc_g = \epsilon/D_g$, to be one. Then, the present particle Schmidt number is simply the ratio of the fluid to particle eddy diffusivity. This ratio was analyzed by Tchen (1947) and by others previously, and the results are summarized in Hinze (1975). As in almost all statistical turbulence analyses, Tchen's work assumed a homogeneous turbulence field. It is known, however, that much of the results of the homogenous turbulence analyses are applicable to shear flows (Hinze, 1975, p. 350). It is expected that Tchen's analysis will give a correct order of the particulate Schmidt number for the present buffer layer.

From the Tchen's analysis,

$$Sc^{-1} = 1 + \left[\frac{1}{(\tau_f/\tau_p)^2 - 1}\right]\left[\frac{\exp(-t/\tau_p) - \exp(-t/\tau_f)}{1 - \exp(-t/\tau_f)}\right]. \tag{17}$$

In this equation, τ_p is the relaxation time of the particle velocity with the fluid viscosity. It is given by

$$\tau_p = \frac{\delta_p d_p^2}{18\mu}, \tag{18}$$

and will be called simply the particle relaxation time. The symbol τ_f denotes the turbulence time scale and is of the order of the characteristic fluctuation time of the energy-containing eddies in the buffer layer. The symbol t denotes particle residence time.

The Cunningham correction factor is neglected in Eq. 18 for the following reasons. First, its effects on τ_p for particles larger than 2 μm is of the order of 1%. For the submicron-size particles, the correction factor is significant; however, $\tau_p/\tau_f \ll 1$, the particles follow the gas turbulence motion independently of the actual value of τ_p/τ_f.

To adapt Tchen's expression of Eq. 17 to the present problem, certain limiting behavior of this equation will be discussed; subsequently, an expression most applicable to solution of the present problem will be deduced.

For $t \ll \tau_p$ and $t \ll \tau_f$, Eq. 17 degenerates to

$$Sc^{-1} = \frac{\tau_f}{\tau_f + \tau_p}. \tag{19}$$

This relationship will be subsequently exploited in evaluating the momentum imparted to the particles to carry them through the laminar sublayer.

At the other extreme of $t \gg \tau_p$ and $t \gg \tau_f$, Eq. 17 gives

$$Sc^{-1} = 1. \tag{20}$$

In this long residence time limit, the particle motion is completely equilibrated to that of the fluid.

In a shear-generated turbulent flow field, such as the buffer layer, the thickness of the shear layer is of the order of the size of the energy-containing eddies (Chung, 1969). Therefore, the residence time of the fluid in the buffer layer is of the order of τ_f. Therefore,

for $t \simeq \tau_f$, but for all finite τ_p, Eq. 17 becomes

$$Sc^{-1} = 1 + \frac{\exp\left(-\frac{\tau_f}{\tau_p} + 1\right) - 1}{1.72\left[\left(\frac{\tau_f}{\tau_p}\right)^2 - 1\right]}. \tag{21}$$

Two limiting values of the ratio, τ_p/τ_f, are considered below for $t \simeq \tau_f$. Equation 21 gives for $\tau_p/\tau_f \ll 1$ (very small and light particles)

$$\frac{D}{\epsilon} \to 1, \tag{22}$$

whereas, for $\tau_p/\tau_f \gg 1$, (very large and heavy particles)

$$\frac{D}{\epsilon} \to 0. \tag{23}$$

Equation 22 shows that small and light particles follow turbulent fluid fluctuations and that, therefore, their particulate diffusivity is identical to the gas eddy diffusivity. On the other hand, large and heavy particles are oblivious to the turbulent fluid fluctuations. It is apparent, therefore, that Eq. 21 is consistent with the expected physical limits regarding particle size and material density.

Having established the expression for Sc, the particle eddy diffusivity is obtained as,

$$D = \epsilon/Sc, \tag{24}$$

where ϵ is given by the usual mixing-length theory as follows.

In the voluminous available information on ϵ, the following expression is given after Cebeci and Chang (1978) for the logarithmic velocity profile in the buffer layer.

$$\epsilon = 0.4\, v_*(y + k_s)\{1 - \exp[-(y + k_s)/A]\}^2, \tag{25}$$

where v_* is the friction velocity, defined by

$$v_* = \sqrt{\tau_w/\rho}. \tag{26}$$

For pipe flow, the following expression found in White (1974) may be used to relate the surface roughness, k_s, to the friction factor, fr.

$$\frac{1}{\sqrt{fr}} = 2.0 \log_{10}\left[\frac{Re\sqrt{fr}}{1 + 0.1\left(\frac{k_s}{d}\right)Re\sqrt{fr}}\right] - 0.8. \tag{27}$$

The friction factor is related to the friction velocity by

$$fr = 2\left(\frac{v_*}{u_a}\right)^2. \tag{28}$$

With Eq. 25, Eq. 24 gives D. Equation 12 then becomes,

$$\hat{D}(y) = 0.4\,\frac{v_*}{Sc}\left\{\int_{(S+k_s)/A}^{(y+k_s)/A} \frac{d\zeta}{\zeta(1 - \exp(-\zeta))^2}\right\}^{-1}. \tag{29}$$

The integral may be evaluated by using the approximation,

$$\frac{1}{\zeta[1 - \exp(-\zeta)]^2} \approx \frac{0.92}{\zeta} + \frac{0.50}{\zeta^2} + \frac{1.08}{\zeta}, \tag{30}$$

valid for $0.1 \leq \zeta \leq 2.5$. Evaluating Eq. 29 at $y = b$ for $b \gg S$, $D(b)$ becomes,

$$\hat{D}(b) = 0.4\,\frac{v_*}{Sc}\Bigg/\left\{0.92\, ln\left(\frac{b^+ + k_s^+}{S^+ + k_s^+}\right) + \frac{13}{S^+ + k_s^+} + \frac{365}{(S^+ + k_s^+)^2}\right\}, \tag{31}$$

where

$$(\,)^+ = \frac{(\,)v_*}{\nu}. \tag{32}$$

This completes the analysis of particulate diffusion across the turbulent buffer layer, and results in the expression for $\hat{D}(b)$. For a given surface roughness, the transcendental Eq. 27 can be solved for fr, from which v_* can be obtained. Particle Schmidt number Sc is given by Eq. 21, where particle relaxation time τ_p is given by Eq. 18. The symbol τ_f is the mean turbulent fluctuation time for the buffer layer, which may be obtained as the ratio of the buffer layer thickness to the mean turbulence velocity in the layer (Hinze, 1975, p. 56).

S, as well as V, will be defined in the next section on discussion of the migration toward wall of the particles through the wall layer.

TURBULENCE-IMPARTED MOMENTUM

Consider that a momentum, m_pV, is imparted to a particle in a quiescent fluid. The distance the particle travels before coming to halt, S, is

$$S = V\tau_p. \tag{33}$$

This distance was defined as the "stopping distance" by Friedlander and Johnstone (1957). Because the turbulent velocity is negligible in the laminar sublayer, only those particles with V, imparted to them by turbulence before reaching the laminar sublayer, such that

$$V > l/\tau_p \tag{34}$$

will arrive at the wall. This inequality shows that the smaller the particles, the greater is the V required for their deposition at the wall. Thermophoresis could, however, cause migration of the small particles to the wall, as will be discussed in the next section.

Returning to the particles that satisfy the inequality of Eq. 34, consider the *rms* radial particulate velocity, V, at S, induced by turbulent fluctuations. The diffusivities for diffusion time (residence time) much shorter than τ_f are proportional to the mean square of velocity fluctuations (Hinze, 1975). The *rms* velocity may be expressed by

$$V = \left[v_r'\left(\frac{1}{Sc}\right)^{1/2}\right]_s \text{ for } \tau \ll \tau_f \tag{35}$$

The radial component of turbulence velocity, v_r', decreases rapidly very close to the wall (for instance, Hinze, 1975). Therefore, for the suddenly decreased local value of v_r', S_c^{-1} of Eq. 35 should be that corresponding to very small t given by Eq. 19. Equation 35 is now written as

$$V = \left[v_r'\left(\frac{\tau_f}{\tau_f + \tau_p}\right)^{1/2}\right]_l. \tag{36}$$

Because S is of the order of l, v_r' and τ_f would be specified at l, instead of S, for convenience.

Equations 33 and 36 define S and V in terms of τ_p given by Eq. 18 and the known near-wall fluid turbulence properties, v_r' and τ_f. With the S determined, and the Sc obtained in the preceding section, Eq. 31 gives $\hat{D}(b)$. Then V, along with the $\hat{D}(b)$, can be used for numerical evaluation of c_a from Eq. 15 and the deposition rate from Eq. 16.

THERMOPHORESIS

When the inequality of Eq. 34 is not satisfied, the turbulence-imparted momentum is insufficient for particle deposition. However, an appropriate temperature gradient could cause particulate transport to the wall by thermophoresis.

Interactions between particles and the surrounding gas molecules in the presence of temperature nonuniformity result in a thermophoretic force on the particles (Tong and Bird, 1970; Jacobsen and Brock, 1965; Brock, 1962; Springer, 1970; Derjarguin and Yalamov, 1965; Brock, 1967). However, attempts to predict the particulate deposition rate from turbulent gas streams have been less than successful, as indicated by Friedlander and Johnstone (1957), Davies (1966), and Byers and Calvert (1969). We feel that the main reason for this lack of success is the inadequacies of the manner in which the thermophoretic principles have been applied to the analysis of particulate deposition from the turbulent gas streams. A method different from those used by previous investigators is used here to analyze the thermophoretic deposition of particles.

By integrating over the particle surface the momentum exchange between the surrounding molecules and the particle, the following equation for the thermophoretic force, F_t, is derived (Jacobsen and Brock, 1965).

$$F_t = -12\pi\mu r_p f(Kn)\frac{\partial T}{\partial y} \tag{37}$$

where

$$f(kn) = \frac{r_p C_{tm} Kn\left\{\left(\frac{k_g}{k_p} + C_t Kn\right)\left(1 + \frac{4}{3}a_3 C_m Kn\right) - \frac{4}{3}a_3 C_m Kn\right\}}{(1 + 3\,C_m Kn)\left(1 + 2\frac{k_q}{k_p} + 2C_t Kn\right)}. \tag{38}$$

Analogously to the description of ion motion in the continuum plasma given in Chung et al. (1975), a particle mobility, B, is defined in such manner that the thermophoretic diffusion velocity, u_t, is given by,

$$u_t = BF_t. \tag{39}$$

The mobility can be expressed from the known drag relationship (Hidy and Brock, 1970) for a spherical particle as,

$$B = g(Kn)/(6\pi\mu r_p), \tag{40}$$

where the Cunningham correction factor $g(Kn)$ is given by

$$g(Kn) = 1 + Kn[1.257 + 0.4\exp(-1.1/Kn)]. \tag{41}$$

Combining Eqs. 37 and 39, we obtain

$$u_t = 2g(Kn)f(Kn)\frac{\partial T}{\partial y}. \tag{42}$$

The temperature gradient that appears in Eq. 42 is replaced by that in the laminar sublayer as,

$$\frac{\partial T}{\partial y} \sim \frac{T_l - T_w}{l}. \tag{43}$$

Before this expression is substituted into Eq. 42, it is put into a more general form by using certain universal properties of turbulent boundary layers, as follows.

First, the laminar sublayer thickness can be expressed in terms of the friction velocity, v_*, as (Schlichting, 1968),

$$l \approx 6\frac{\nu}{v_*}. \tag{44}$$

Then, employing the Reynolds analogy,

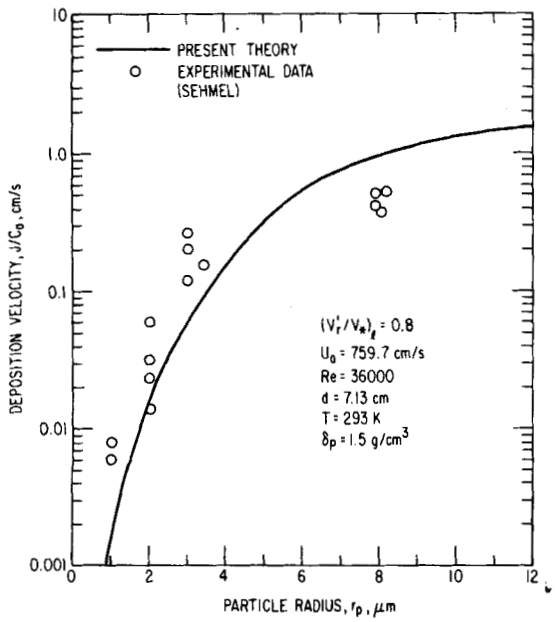

Figure 2. Variation of deposition velocity with respect to particle radius for isothermal flow.

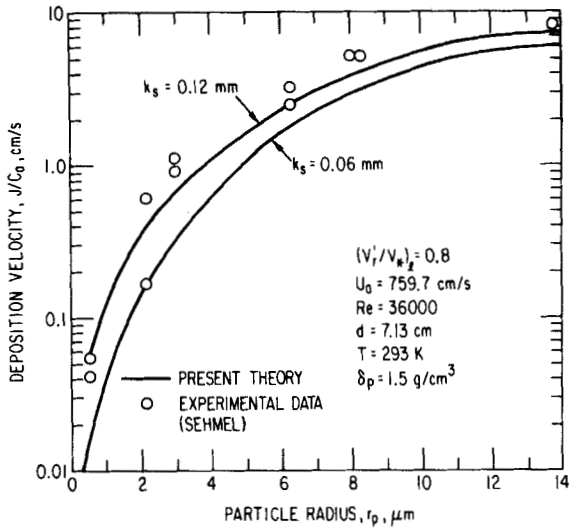

Figure 3. Variation of deposition velocity with respect to particle radius and wall surface roughness for isothermal flow.

$$T_l - T_w = 6\left(\frac{fr}{8}\right)^{1/2}(T_a - T_w). \tag{45}$$

Using Eqs. 43 and 44, Eq. 42 becomes,

$$u_t = 2\left(\frac{fr}{8}\right)^{1/2}\frac{v_*}{\nu}g(Kn)f(Kn)(T_a - T_w). \tag{46}$$

At the laminar sublayer edge, $y = l$,

$$V = u_t. \tag{47}$$

With l substituted for S and $Sc = 1$ (Eq. 22), $\hat{D}(b)$ is given by Eq. 31. With V and $\hat{D}(b)$ known, Eqs. 15 and 16 give the particulate deposition rate when $S < l$.

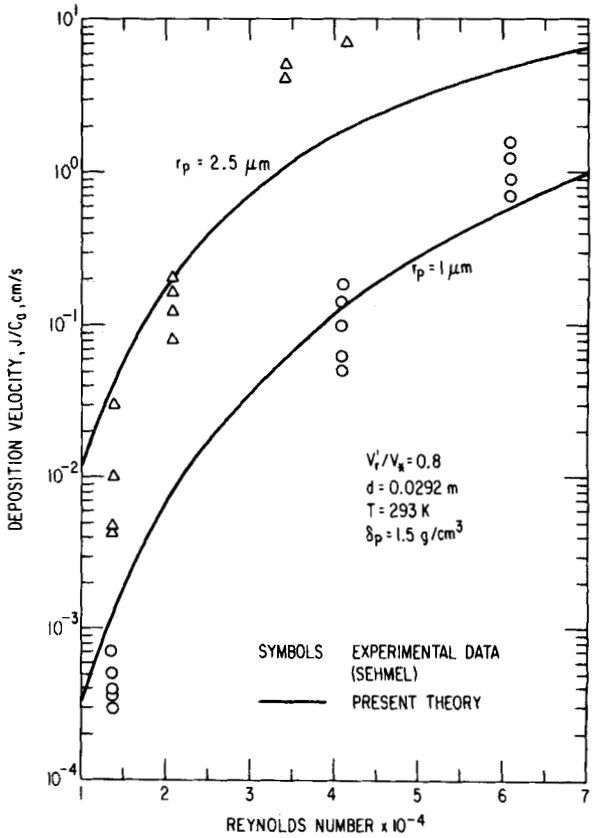

Figure 4. Variation of deposition velocity with respect to Reynolds number an particle radius for isothermal flow.

RESULTS AND DISCUSSION

A number of experimental results found in the literature can be used to test the present theory. Data are presented in Sehmel (1968), Friedlander and Johnstone (1957), and Wells and Chamberlain (1967), such that the deposition velocity, J/c_a, given by Eq. 16 can be compared directly. The theoretical curves shown in Figures 2 through 6 have been constructed from Eqs. 16, 31, 33 and 36 for environments corresponding to the experiments. The values of v_r'/v_* at the laminar sublayer edge for the given Reynolds number ranges were estimated from Hinze (1975). These experiments were conducted in an isothermal environment so that the thermophoresis was inactive. Rather wide ranges of particle size, Reynolds number, and τ_p are covered in these figures. The present theory agrees satisfactorily with the experimental data. In particular, the theory predicts variation of the deposition rate with respect to the particle size, Reynolds number, and particle relaxation time quite accurately.

The theoretical prediction of Friedlander and Johnston (1957) is shown in Figure 5, along with their experimental data. It seems that the present theory agrees more closely with the experimental findings than the theory of Friedlander and Johnston.

Variation of the dimensionless deposition velocity with respect to dimensionless relaxation parameter is shown in Figure 6, which is reconstructed from Chamberlain's result (1969). The experimental data of Wells and Chamberlain (1967) and Sehmel (1968), and the theoretical predictions of Kneen and Strauss (1969), Davies (1965), and the present authors are the bases of the figure. The present theory predicts an exponential variation of the deposition velocity with respect to τ_p, as do Kneen and Strauss.

In Figures 2–4, the triangles and circles refer to experimental data of Sehmel (1968). In the experiments of Sehmel, particles of uranine or uranine-methylen blue were in narrow size ranges, prepared using a spinning disc generator. The deposition on the tube surface was measured either by washing the entire length of the tube or by cutting the tube into short lengths, then washing the segments separately. The segmented washing allows local measurements of the deposition rates. It is evident from Figures 2 and 3 that the deposition rate increases with the particle size up to order of 10 μm for the material density considered. This is because the larger particles are able to retain the turbulence-imparted momentum longer than the smaller ones, as indicated by Eq. 33. The deposition rate, however, levels off and will eventually decrease to zero, as the particle size is continuously increased. This is due to the fact that an increasingly smaller portion of the fluid turbulence momentum can be imparted to the solid particles as they become larger. Eventually, a point is reached where practically no fluid momentum can be imparted to the particle near the wall. The momentum retention capacity of the particle, then, is a moot point. This behavior of deposition rate with respect to the particle size is evident in Eqs. 16, 31, 33 and 36.

Figure 3 shows that the deposition rate is substantially influenced by the roughness of the collector surface. As indicated in Eqs. 25–31, the surface roughness directly affects the fluid turbulence level near the wall. Therefore, it is expected to affect the deposition rate substantially.

A higher Reynolds number implies a higher turbulence level in a pipe flow. Therefore, the larger Reynolds numbers result in the greater deposition rate, Figure 4. This increase in the deposition rate with the increasing Re is monotonic.

The results for thermophoretic deposition are presented in Figures 7 and 8. Present theoretical results are compared with the experimental data of Byers (1967). In his experiment, the droplets of a 10% sodium chloride water solution, formed by atomization, were dried to sodium chloride particles. The test section consisted of a water-jacketed copper tube. The particle-ladden hot gas was passed through the test section, and the particle concentrations were measured at two different stations. The collection efficiency is shown, which is the total deposition rate in the pipe expressed as percentage of the particulate flow rate into the pipe. The theo-

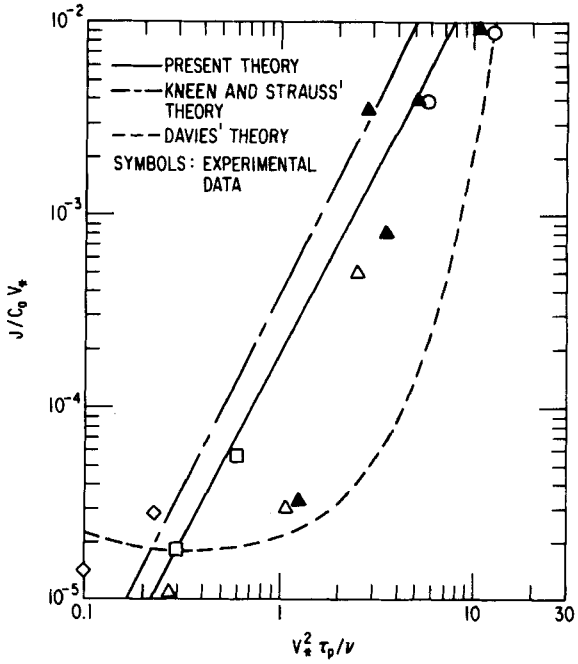

Figure 6. Relationship between dimensionless deposition velocity and dimensionless particle relaxation time for isothermal flow.

Ref.	Symbol	r_p	δ_p (g/cm^3)	10^{-4} Re
Wells and Chamberlain	◇	0.33	1.2	3.0-4.7
Wells and Chamberlain		0.55	1.2	3.0-4.7
Wells and Chamberlain	△	1.5	1.2	1.3-4.7
Wells and Chamberlain	○	2.5	1.0	1.3-4.7
Sehmel	△	1.0	1.5	0.5-1.7

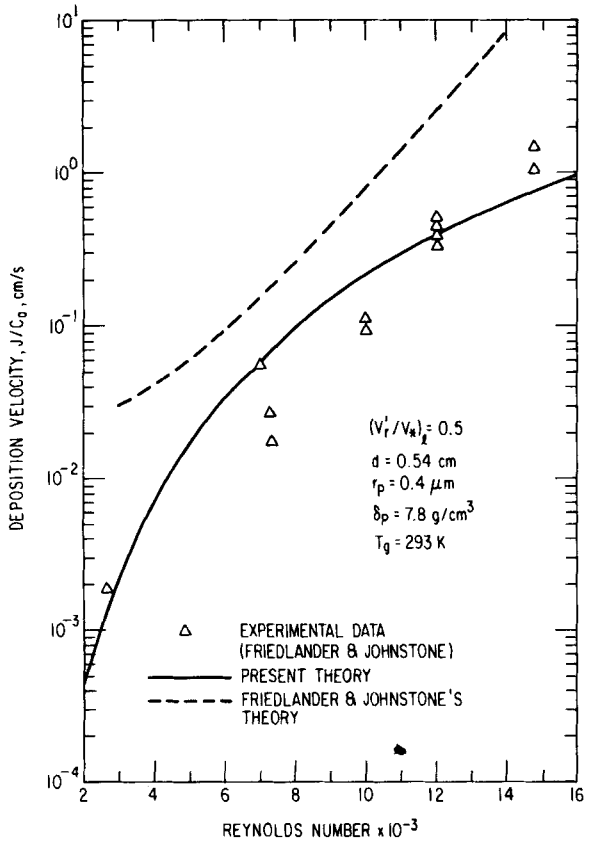

Figure 5. Variation of deposition velocity with respect to Reynolds number for isothermal flow.

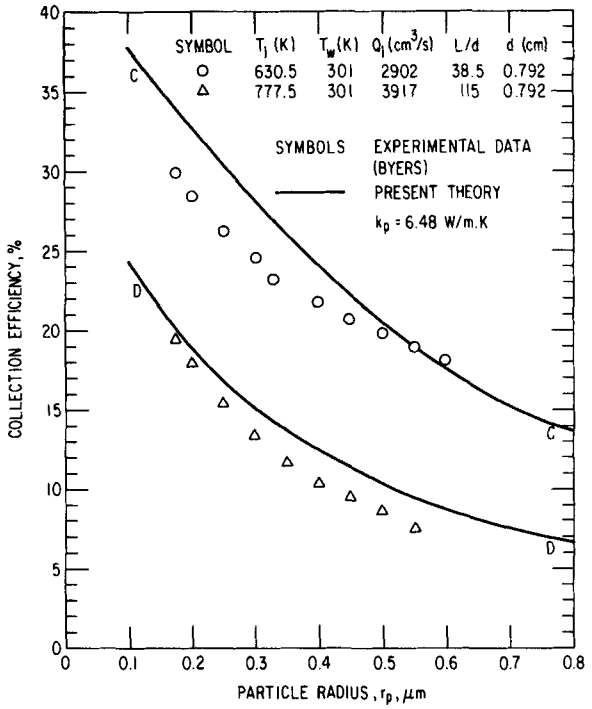

Figure 7. Variation of thermophoretic collection efficiency with respect to particle size.

retical curves are constructed from the numerical solutions of Eq. 16 with the aid of Eqs. 31 and 47. Satisfactory agreements with the experimental data are indicated. Thermophoresis is shown to be an effective mechanism for particulate deposition when the particles are less than ~1 μm in radius.

The two sets of data shown in Figure 8, represented by the squares and inverted triangles respectively, are obtained essentially for the same experimental condition, except for the different temperature differences between the fluid and the pipe wall. Dominant influence of the temperature difference on the deposition efficiency is seen.

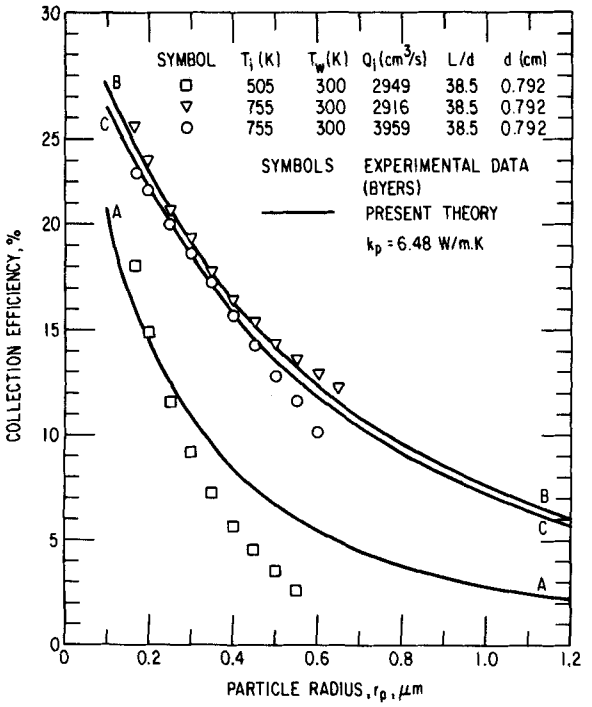

Figure 8. Variation of thermophoretic efficiency with respect to particle size and temperature difference.

NOTATION

A = constant for eddy viscosity ($A = 26\,\nu/v^*$)
a_3 = constant associated with second order slip = 2.4
B = mobility of a particle, m/(s·N)
b = buffer layer thickness ($b = 100\,\nu/v^*$)
C_m = viscous slip coefficient = 1.19
C_t = temperature jump coefficient = 3.32
C_{tm} = thermal velocity coefficient = 0.461 m/(s·K)
c = concentration of particles, kg/m^3
D = particulate eddy diffusivity, m^2/s
$\hat{D}$ = effective turbulent diffusion velocity, m/s
d = pipe diameter, m
d_p = particle diameter, m
F = function defined by Eq. 12, m^2/s
F_t = thermophoretic force, N
$f(Kn)$ = function defined by Eq. 36, m^2/s
fr = friction factor defined by Eq. 26
$g(Kn)$ = Cunningham correction factor defined by Eq. 39
J = particle flux toward the surface at S, kg/(s·m^2)
Kn = Knudsen Number, λ/r_p
k_g = thermal conductivity of gas, W/(m·K)
k_p = thermal conductivity of particle, W/(m·K)
k_s = effective collector surface roughness, m
l = laminar sublayer thickness, ($l = 6\,\nu/v^*$)
r_p = particle radius
R = pipe radius, m
Re = Reynolds number, $\bar{u}d/\nu$
r = radial coordinate, m (Figure 1)
S = stopping distance, m
Sc = particulate Schmidt number, ϵ/D
T = temperature, K
t = time, s
u = streamwise velocity, m/s
u_t = thermophoretic velocity, m/s
V = rms radial particle velocity at S, m/s
v_* = friction velocity defined by Eq. 24, m/s
v_r = rms radial component of turbulence velocity, m/s
x = streamwise coordinate, m (Figure 1)
y = normal distance measured from the surface, m (Figure 1)

Greek Letters

δ_p = material density of the particles, kg/m^3
ϵ = eddy viscosity of gas, m^2/s
ζ = dummy variable
λ = gas mean free path
μ = dynamic viscosity of gas, N·s/m^2
ν = kinematic viscosity of gas, m^2/s
ρ = gas density, kg/m^3
τ_p = particle relaxation time, s
τ_f = turbulent integral time scale, s
τ_w = shear stress at wall, N/m^2

Subscripts

a = turbulent core of flow
b = buffer layer edge
l = laminar sublayer edge
s = stopping distance
w = collector wall
o = at $x = o$

LITERATURE CITED

Ahluwalia, R. K., and E. Doss, "Convective Heat Transfer in MHD Channels and Its Influence on Channel Performance," *J. of Energy*, 4, 126 (1980).

Brock, J. R., "On the Theory of Thermal Force on Aerosol Particles," *J. Colloid and Interface Sci.*, **17**, 768 (1962).
Brock, J. R., "The Thermal Force in the Transition Region," *J. Colloid and Interface Sci.*, **23**, 448 (1967).
Bueters, K. A., "Performance Prediction of Tangentially Fired Utility Furnaces by Computer Model," 15th Int. Symp. on Comb. (1974).
Byers, R. L., and S. Calvert, "Particle Deposition from Turbulent Streams by Means of Thermal Force," *I&EC Fund.*, **8**, 646 (1969).
Byers, R. L., "Particle Deposition from Turbulent Streams by Means of Thermal Force," Ph.D. Thesis, The Pennsylvania State University (1967).
Cebeci, T., and K. C. Chang, "Calculation of Rough-wall Boundary Layer Flows," *AIAA J.*, **16**, 730 (1978).
Cebeci, T., and A. M. O. Smith, *Analysis of Turbulent Boundary Layers*," Chapter 6, Academic Press, New York (1974).
Chamberlain, A. C., "Deposition of Dust from Turbulent Gas Stream," *Atmos. Environ.*, **3**, 494 (1969).
Chung, P. M., L. Talbot, and K. Touryan, *Electric Probes in Stationary and Flowing Plasma; Theory and Applications*, Spring-Verlag, New York (1975).
Chung, P. M., "A Simplified Statistical Model of Turbulent Chemically Reacting Shear Flow," *AIAA J.*, **7**, 1982 (1969).
Davies, C. N., "Deposition of Aerosols from Turbulent Flow Through Pipes," *Proc. Roy. Soc.*, **A289**, 235 (1966).
Derjarguin, B. V., and Yalamov, Y., "Theory of Thermophoresis of Large Aerosol Particles," *J. Colloid. Sci.*, **20**, 555 (1965).
Friedlander, S. K., and H. F. Johnstone, "Deposition of Suspended Particles from Turbulent Gas Stream," *Ind. Eng. Chem.*, **49**, 1151 (1957).
Fuchs, N. A., *The Mechanics of Aerosols*, Chapter 5, Pergamon Press, New York (1964).
Hidy, G. M., and J. R. Brock, *The Dynamics of Aerocolloidal Systems*, Pergamon Press, New York (1970).
Hinze, J. O., *Turbulence*, Chapter 5, McGraw Hill Book Co., New York (1975).
Jacobsen, S., and J. R. Brock, "The Thermal Force on Spherical Sodium Chloride Aerosols," *J. Colloid. Sci.*, **20**, 544 (1965).
Kneen, T., and W. Strauss, "Deposition of Dust from Turbulent Gas Streams," *Atmos. Environ.*, **3**, 55 (1969).
Schlichting, H., *Boundary Layer Theory*, McGraw-Hill Book Co., New York (1968).
Sehmel, G. A., "Aerosol Deposition from Turbulent Airstreams in Vertical Conduits," *Health and Safety*, BNWL-578, UC-14 (1968).
Springer, G. S., "Thermal Force on Particles in the Transition Regime," *J. Colloid. Sci.*, **34**, 215 (1970).
Tchen, C. M., "Mean Value and Correlation Problems Connected With the Motion of Small Particles Suspended in a Turbulent Fluid," Ph.D. Thesis, Delft (1947).
Tong, N. T., and G. A. Bird, "Thermal Force in the Low Density Limit," *J. Colloid. and Interface Sci.*, **35**, 403 (1971).
White, F., *Viscous Fluid Flow*, Chapter 6, p. 491, McGraw Hill Book Co., New York (1974).
Wells, A. C., and A. C. Chamberlain, "Transport of Small Particles to Vertical Surfaces," *Brit. J. Appl. Phys.*, **18**, 1793 (1967).

Manuscript received October 23, 1981; revision received May 25, and accepted June 18, 1982.